Biomedical Signal Processing and Control 91 (2024) 105994

Contents lists available at ScienceDirect

Biomedical Signal Processing and Control

journal homepage: www.elsevier.com/locate/bspc

# Computational dynamics of a fractional order model of chickenpox spread in Phuket province

Sayooj Aby Jose [a,b], Zakaria Yaagoub [c], Dianavinnarasi Joseph [d], Raja Ramachandran [e,f], Anuwat Jirawattanapanit [b,*]

[a] Department of Mathematics, Alagappa University, Karaikudi 630 003, India
[b] Department of Mathematics, Faculty of Education, Phuket Rajabhat University, Phuket, Thailand
[c] Laboratory of Mathematics, Computer Science and Applications, Faculty of Sciences and Technologies, University Hassan II of Casablanca, PO Box 146, Mohammedia 20650, Morocco
[d] Centre for Nonlinear Systems, Chennai Institute of Technology, Chennai 600069, Tamil Nadu, India
[e] Ramanujan centre for Higher Mathematics, Alagappa University, Karaikudi 630 003, India
[f] Department of Computer Science and Mathematics, Lebanese American University, Beirut, Lebanon

ARTICLE INFO

*Keywords:*
Chickenpox
Caputo fractional derivative
Precautionary measures
Exponentiating the parameters
Reproduction number

ABSTRACT

In this investigation, a distinctive chickenpox model incorporating the Caputo fractional derivative is introduced. Equilibrium points and the fundamental reproduction number of the model are systematically computed. The study also scrutinizes the existence, uniqueness, positivity, and boundedness of solutions. Furthermore, a comprehensive analysis of both local asymptotic stability and global stability at the disease-free equilibrium is carried out. To demonstrate the practical utility of the model, a numerical simulation of chickenpox dynamics in Phuket city is conducted using MATLAB. This research contributes to a better understanding of chickenpox transmission dynamics, offering valuable insights for disease control and management strategies.

## 1. Introduction

*Varicella-Zoster Virus* (VZV), sometimes referred to us the "Chickenpox virus", is an extremely infectious illness that affects exclusively humans. The virus can last for hours in a typical setting [1]. The *Herpes Simplex Virus* (HSV) is a part of the human herpesvirus family, which also includes the VZV, a closely related but separate component. The cause of two distinct illnesses is VZV. Varicella, often known as chickenpox, is the primary source of infection and is a communicable disease. The reactivation of VZV from an inactive condition causes shingles, or zoster, which is its secondary disease. Most people get varicella at some time in their lives. The VZV enters a latent condition after the initial Varicella occurrence and frequently stays dormant for a long time without exhibiting any symptoms. Nonetheless, the VZV may reactivate and result in the development of zoster in 20% of individuals. Immunocompromised and elderly individuals are more likely to have reactivation [2,3].

The fact that VZV causes approximately 10,000 fatalities each year is a particularly significant concern [2]. Before the vaccine's discovery in 1995, there were annual records of 4 million varicella cases and 1 million zoster cases, with the disease's spread being influenced by geographical factors [4]. Varicella is typically diagnosed in children, while shingles or zoster is more commonly found in adults. This virus used to infect nearly everyone worldwide due to its rapid transmission before the development of vaccines [5].

Adults become resistant to VZV in temperate nations like the United States and the United Kingdom [6]. Preblud's study in [7] found that, in America at least 90% of people at the age of 15, had been infected with the virus. Muench et al. found 100% seropositivity at age 13 in a research conducted in Seattle in that same year [7,8]. According to Wharton's study, only 6% of people between the ages of 11 and 19 were at risk of contracting VZV infection [9]. Only 6.7% of recruits for the U.S. Navy and Marine Corps, aged 15 to 29, tested negative for VZV, according to [10]. [6] has the review of Chicken Box in its entirety.

Compared to integer-order calculus, fractional calculus provides a more natural way to comprehend different facets of life. It is an effective analytical technique for explaining historical behaviors, intricate systems, and interconnections. Fractional-order partial differential equations (PDEs) are a major component of many models in disciplines such as fluid dynamics, electricity, ecology, and quantum physics. In order to tackle contemporary scientific problems, a thorough understanding of integrals and derivatives, both fractional and integer, is required. These mathematical tools are notable for their ability to be used with unique functions such as Gamma and Beta, and for convolutions in integrals.

* Corresponding author.
*E-mail address:* anuwat.j@pkru.ac.th (A. Jirawattanapanit).

https://doi.org/10.1016/j.bspc.2024.105994
Received 6 November 2023; Received in revised form 23 December 2023; Accepted 29 January 2024
1746-8094/© 2024 Elsevier Ltd. All rights reserved.

Fractional Differential Equations (FDEs) offer more insights on the suggested scenario's memory and heredity. Ellipstic functions, elliptic integrals, and special functions are utilized in a number of biological systems [11]. They are well understood to be involved in the solution of nonlinear differential equations. These days, FDEs are robust, rigorous computational tools that may be used to analyze a variety of ecological and technological phenomena [12].

Further information on the disease's heredity can be obtained by analyzing a mathematical model in the fractional order sense. For example, the authors of [13–20] used fractional and integer calculus to study the nonlinear dynamics of prevalent childhood disorders, mosquito borne disease control and they used the Adams–Bashforth method, RH criterion and Lyapunov theory for numerical simulations. More importantly, asymptotic behaviors of chikungunya are examined in [21], hepatitis C model with Mittag-leffler kernel is described in [22], and fractional calculus is used in the coronary heart disease model [23]. In [5], the authors created a compartmental model of Chicken box virus transmission in order to study the impact of the varicella-zoster vaccination. They did this by using the notion of $ABC-$ fractional derivative. The paper by Sayooj et al. [24], introduces the Integer ordered Chickenpox Model, which aims to investigate the impact of implementing preventive measures among individuals who are infected. In their study, the authors analyze the proposed model using real-world data collected from Phuket province, Thailand. In light of the findings presented above, our article makes the following significant contributions to the understanding and control of VZV transmission as categories:

(i) *Model Development:* We proposed a novel fractional order mathematical model to understand the spread of Chickenpox in Phuket city, Thailand by incorporating the concept of parameter exponentiation. This model deepens our comprehension of the disease's progression mechanisms.
(ii) *Model Characteristics:* We establish the positive invariant region and address the existence and uniqueness of the model, thereby confirming the validity of our infection modeling approach.
(iii) *Disease Dynamics:* We analyze disease transmission dynamics in individuals with and without complications at varying fractional order levels, providing valuable insights into the disease's behavior that the infection rate in population with complication is higher than that of population without complications. Furthermore, the existence and uniqueness of solution is derived analytically.
(iv) *Equilibrium Points:* We investigate the equilibrium points of the proposed model. The next generation matrix method is utilized to find the corresponding reproduction number to assess their local and global dynamics using Lapunov's method and LaSalle's invariance principle.
(v) *Preventive Measures:* We demonstrate that by implementing different levels of precautionary measures, the basic reproductive number within fractional orders can be significantly reduced, contributing to disease control. We analyzed the reality of the model by examine it in various cases. That is, in numerical simulation we analyzed the model in presence and absence of vaccination while the parameters are exponentiated and not exponentiated.
(vi) *Memory Effect Analysis:* Through numerical analysis, we explore the impact of the memory effect on dynamical behaviors by examining the influence of derivative orders. From numerical analysis, the importance of considering parameter exponentiation is presented.

These contributions collectively enhance our understanding of VZV transmission and offer insights into effective strategies for controlling its spread.

The manuscript is organized as follows: In Section 2, we introduce a novel fractional-order model by raising it to the power of the fractional-order derivative $\alpha$. Section 3 is dedicated to the analysis of qualitative properties, specifically examining aspects such as positivity and boundedness of the solutions. Section 4 is where we derive the reproduction number at the model's equilibrium points. Furthermore, in Section 5, we establish the global stability of these equilibrium points through the application of Lyapunov stability theory and Lasalle's invariance principle. Section 6 is designated for the numerical analysis of the model, where we incorporate field data collected from Phuket province, Thailand. In Section 8, we provide the comparison results which shows the effectiveness of vaccination. Finally, in Section 8, we provide our concluding remarks based on the obtained results.

## 2. Motivation and model formation

Fractional derivatives have emerged as a compelling approach to model disease epidemics more realistically. This stems from their unique capacity to incorporate memory effects, which are frequently observed in the human body's response to diseases. These memory effects account for the persistence of immunity, the temporal dynamics of infections, and other intricate characteristics of epidemics. In light of this, we present an innovative extension of the traditional chickenpox model. By introducing fractional orders into this model, we aim to more accurately capture the intricate dynamics and memory-dependent aspects of chickenpox epidemics. This extension allows us to explore the long-term behavior of the disease, examine the impact of Precautionary Measures, and provide insights into the potential for outbreak control strategies. We have examined the mathematical framework presented in [24] and incorporated the notion of parameter exponentiation within the fractional-order model in the Caputo sense, as follows:

$$\begin{aligned}
D_t^\alpha C_S(t) &= \Lambda^\alpha - \lambda_1^\alpha C_S(C_{IW} + \eta^\alpha C_{I\overline{W}}) + \lambda_3^\alpha C_V \\
&\quad + \mu^\alpha C_E - (\gamma^\alpha + \lambda_2^\alpha) C_S + \psi_3^\alpha C_R \\
D_t^\alpha C_V(t) &= \lambda_2^\alpha C_S - (1-\theta)\lambda_1^\alpha C_{IW} C_V - (1-\theta)\lambda_1^\alpha \eta^\alpha C_{I\overline{W}} C_V \\
&\quad - (\lambda_3^\alpha + \gamma^\alpha) C_V \\
D_t^\alpha C_E(t) &= (1-\theta)\lambda_1^\alpha C_{IW} C_V + (1-\theta)\lambda_1^\alpha \eta^\alpha C_{I\overline{W}} C_V \\
&\quad + \lambda_1^\alpha C_S(C_{IW} + \eta^\alpha C_{I\overline{W}}) - (\lambda_4^\alpha + \gamma^\alpha + \mu^\alpha) C_E \\
D_t^\alpha C_{IW}(t) &= \vartheta \lambda_4^\alpha C_E - (\psi_1^\alpha + \gamma^\alpha + \gamma_1^\alpha) C_{IW} \\
D_t^\alpha C_{I\overline{W}}(t) &= (1-\vartheta)\lambda_4^\alpha C_E - (\psi_2^\alpha + \gamma^\alpha + \gamma_2^\alpha) C_{I\overline{W}} \\
D_t^\alpha C_R(t) &= \psi_1^\alpha C_{IW} + \psi_2^\alpha C_{I\overline{W}} - (\gamma^\alpha + \psi_3^\alpha) C_R.
\end{aligned} \tag{1}$$

Here, we propose a novel fractional order variant of the chickenpox model (1), which promises to enhance our understanding of chickenpox epidemics and contribute to the development of more effective disease management strategies. In this context, we represent the city as $C$, with its population divided into distinct groups: the susceptible population in the city is denoted as $C_S$, vaccinated population as $C_V$, the people who are exposed to the infection is denoted as $C_E$. Significantly, the infected compartment is partitioned into two major compartments such as infected population with complication $C_{IW}$ and infected population without complication $C_{I\bar{W}}$. The recovered population is denoted as $C_R$. The description of the parameters used in the model is found in Table 1. The initial conditions are, $C_S(0) = C_{S_0} > 0$, $C_V(0) = C_{V_0} \geq 0$, $C_E(0) = C_{E_0} \geq 0$, $C_{IW}(0) = C_{I_0} \geq 0$, $C_{I\overline{W}}(0) = C_{A_0} \geq 0$, $C_R(0) = C_{R_0} \geq 0$. In the preceding context, the symbol $D^\alpha$ represents the Caputo fractional derivative with an order denoted as $0 < \alpha \leq 1$. It is worth mentioning that all the model parameters, with the exception of $\theta$ and $\vartheta$, possess dimensions of $\frac{1}{t^\alpha}$. To maintain dimensional consistency, as emphasized by Ref. [25], we have raised these parameters to the power of $\alpha$.

## 3. Qualitative aspects of solutions

In this section, we explore the mathematical and biological aspects of the fractional order model. Essentially, we establish that when a positive initial condition is provided, the solution to the fractional

**Table 1**
Description of parameters utilized in the proposed model.

| Variables | Description |
|---|---|
| $C_S$ | Susceptible individuals in $C$ |
| $C_V$ | Vaccinated individuals in $C$ |
| $C_E$ | Exposed individuals in $C$ |
| $C_{IW}$ | Infected individuals with complications in $C$ |
| $C_{I\overline{W}}$ | Infected individuals without complications in $C$ |
| $C_R$ | Recovered individuals in $C$ |
| **Parameters** | **Description** |
| $\Lambda$ | Recruitment rate |
| $\lambda_1$ | Disease transmission rate |
| $\eta$ | Modification parameter that accounts for reduced transmission in infected individuals without complications in $C$ |
| $\lambda_3$ | Waning effect |
| $\lambda_2$ | Vaccination rate |
| $\mu$ | precaution taking individuals |
| $\theta$ | Vaccine efficacy |
| $\lambda_4$ | Disease progression rate of infectious of exposed individuals |
| $\vartheta$ | Proportion of individuals to infected individuals with complications |
| $\psi_1$ | Recovery rate of infected individuals with complications |
| $\psi_2$ | Recovery rate of infected individuals without complications |
| $\gamma_1$ | Death rate of infected individuals with complications |
| $\gamma_2$ | Death rate of infected individuals without complications |
| $\gamma$ | Natural death rate of individuals |
| $\psi_3$ | Rate of loss of infection - acquired(natural) immunity |

model remains both bounded and positive. Additionally, we establish the presence of a unique solution for the model.

Let $\Theta(t) = (C_S, C_V, C_E, C_{IW}, C_{I\overline{W}}, C_R)^\top$ and $\mathcal{K}(t, \Theta(t)) = (\Xi_i)^\top,\ i = 1, 2, 3, \dots 6.$

Here,

$$\begin{aligned}
\Xi_1 &= \Lambda^\alpha - \lambda_1^\alpha C_S(C_{IW} + \eta^\alpha C_{I\overline{W}}) + \lambda_3^\alpha C_V + \mu^\alpha C_E - (\gamma^\alpha + \lambda_2^\alpha)C_S + \psi_3^\alpha C_R,\\
\Xi_2 &= \lambda_2^\alpha C_S - (1-\theta)\lambda_1^\alpha C_{IW} C_V - (1-\theta)\lambda_1^\alpha \eta^\alpha C_{I\overline{W}} C_V - (\lambda_3^\alpha + \gamma^\alpha)C_V,\\
\Xi_3 &= (1-\theta)\lambda_1^\alpha C_{IW} C_V + (1-\theta)\lambda_1^\alpha \eta^\alpha C_{I\overline{W}} C_V + \lambda_1^\alpha C_S(C_{IW} + \eta^\alpha C_{I\overline{W}})\\
&\quad - (\lambda_4^\alpha + \gamma^\alpha + \mu^\alpha)C_E,\\
\Xi_4 &= \vartheta\lambda_4^\alpha C_E - (\psi_1^\alpha + \gamma^\alpha + \gamma_1^\alpha)C_{IW},\\
\Xi_5 &= (1-\vartheta)\lambda_4^\alpha C_E - (\psi_2^\alpha + \gamma^\alpha + \gamma_2^\alpha)C_{I\overline{W}},\\
\Xi_6 &= \psi_1^\alpha C_{IW} + \psi_2^\alpha C_{I\overline{W}} - (\gamma^\alpha + \psi_3^\alpha)C_R.
\end{aligned} \tag{2}$$

Next, we can express the dynamical system described by Eq. (1) as follows,

$$D_t^\alpha \Theta(t) = \mathcal{K}(t, \Theta(t)),\ \Theta(0) = \Theta_0 \geq 0,\ t \in [0, m],\ 0 < \alpha \leq 1. \tag{3}$$

In the previous, it should be understood that the condition $\Theta(0) \geq 0$ applies to each component individually. Eq. (2), which is equivalent to the fractional differential equation (1), can be represented as an integral as well.

$$\begin{aligned}
\Theta(t) &= \Theta_0 + \mathcal{I}_{0+}^\alpha \mathcal{K}(t, \Theta(t))\\
&= \Theta_0 + \frac{1}{\Gamma(\alpha)} \int_0^t (t-\varsigma)^{\alpha-1} \mathcal{K}(\varsigma, \Theta(\varsigma)) d\varsigma
\end{aligned} \tag{4}$$

Subsequently, we will examine model (1) using the integral representation provided. To facilitate this, let us define $\Psi$ as the Banach space comprising continuous functions from the interval $[0, m]$ to $\mathbb{R}$ and equipped with its associated norm.

$$\|\Theta\|_\Psi = \sup_{t \in [0,m]} \{ |\ \Theta(t)\ | \},$$

here, $|\ \Theta(t)\ | = |\ C_S\ | + |\ C_V\ | + |\ C_E\ | + |\ C_{IW}\ | + |\ C_{I\overline{W}}\ | + |\ C_R\ |$. Note that $C_S, C_V, C_E, C_{IW}, C_{I\overline{W}}, C_R$ all belongs to $C([0, m]; \mathbb{R})$. Then the operator $\mathcal{Q} : \Psi \longrightarrow \Psi$ by,

$$(\mathcal{Q}\Theta)(t) = \Theta_0 + \frac{1}{\Gamma(\alpha)} \int_0^t (t-\varsigma)^{\alpha-1} \mathcal{K}(\varsigma, \Theta(\varsigma)) d\varsigma. \tag{5}$$

Observe that the operator $\mathcal{Q}$ is well-defined because of the clearly evident continuity of $\mathcal{K}$.

### 3.1. Existence, uniqueness positivity and boundedness of solutions

In this sub-section, we will prove the existence, uniqueness positivity and boundedness of the solutions of the system (2). Let us denote

$$\mathbb{R}_+^6 = \left\{ \left(C_S, C_V, C_E, C_{IW}, C_{I\overline{W}}, C_R\right) | C_S, C_V, C_E, C_{IW}, C_{I\overline{W}}, C_R \geq 0 \right\}.$$

**Theorem 3.1** (*Solution's Existence and Uniqueness*). *Let $t_F \in \mathbb{R}_+^6$. The system (2) has a unique solution on $(0, t_F)$ for initial conditions satisfying $C_S(0) > 0, C_V(0) > 0,\ C_E(0) > 0, C_{IW}(0) > 0, C_{I\overline{W}}(0) > 0, C_R(0) > 0$.*

**Proof.** Let $x(t) = (C_S, C_V, C_E, C_{IW}, C_{I\overline{W}}, C_R)^\top$, then the system (2) translates as $x'(t) = G(x(t)) = \left(g_1(x), g_2(x)g_3(x), g_4(x), g_5(x), g_6(x)\right)^\top$ with $x(0) = \left(C_S(0), C_V(0), C_E(0), C_{IW}(0), C_{I\overline{W}}(0), C_R(0)\right)^\top > 0$.

The elements of Jacobian matrix of $G$, denoted as $J(G(X))$ is given by

$$\begin{aligned}
J_{11} &= \frac{\partial g_1}{\partial C_S} = \lambda_1^\alpha C_S(C_{IW} + \eta^\alpha C_{I\overline{W}}) - (\gamma^\alpha + \lambda_2^\alpha),\\
J_{12} &= \frac{\partial g_2}{\partial C_V} = -(1-\theta)\lambda_1^\alpha C_{IW} - (1-\theta)\lambda_1^\alpha \eta^\alpha C_{I\overline{W}} - (\lambda_3^\alpha + \gamma^\alpha),\\
J_{13} &= \frac{\partial g_3}{\partial C_E} = -(\lambda_4^\alpha + \gamma^\alpha + \mu^\alpha), \quad J_{14} = \frac{\partial g_4}{\partial C_{IW}} = -(\psi_1^\alpha + \gamma^\alpha + \gamma_1^\alpha),\\
J_{15} &= \frac{\partial g_1 5}{\partial C_{I\overline{W}}} = -(\psi_2^\alpha + \gamma^\alpha + \gamma_2^\alpha), J_{16} = \frac{\partial g_5}{\partial C_R} = -(\psi_3^\alpha + \gamma^\alpha), \quad \text{etc.}
\end{aligned}$$

Then $G$ and $J(G(X))$ are continuous for $t > 0$. Due to this, $G$ satisfies a Lipschitz condition on $\mathbb{R}_+^6$. Then from the Picard–Lindelof theorem, we can deduce the existence and uniqueness of solution on $(0, t_F)$. □

**Theorem 3.2.** *Let $\Theta(t) = (C_S, C_V, C_E, C_{IW}, C_{I\overline{W}}, C_R)^\top$. Then for $\Theta_0 > 0$, the solution $\Theta(t)$ of (1) is bounded, and remains positive for $t \geq 0$.*

**Proof.** We begin by confirming the positivity of the solution. From [26], consider the trajectory of solution along the $C_S$-axis where $C_V(0) = C_E(0) = C_{IW}(0) = C_{I\overline{W}}(0) = C_R$ and $C_S(0) = C_{S_0} > 0$. Then $D_t^\alpha C_S(t) = \Lambda^\alpha - (\gamma^\alpha + \lambda_2^\alpha)C_S$, its solution is given by $C_S(t) = C_{S_0}E_\alpha(-(\gamma^\alpha + \lambda_2^\alpha)t^\alpha) + \frac{\Lambda^\alpha}{(\gamma^\alpha + \lambda_2^\alpha)}(1 - E_\alpha(-(\gamma^\alpha + \lambda_2^\alpha)t^\alpha))$. Similar arguments yield,

$$
\begin{aligned}
C_V(t) &= C_V(0)E_\alpha(-(\lambda_3^\alpha + \gamma^\alpha)t^\alpha) > 0,\\
C_E(t) &= C_E(0)E_\alpha(-(\lambda_4^\alpha + \gamma^\alpha + \mu^\alpha)t^\alpha) > 0,\\
C_{IW}(t) &= C_{IW}(0)E_\alpha(-(\psi_1^\alpha + \gamma^\alpha + \gamma_1^\alpha)t^\alpha) > 0,\\
C_{I\overline{W}}(t) &= C_{I\overline{W}}(0)E_\alpha(-(\psi_2^\alpha + \gamma^\alpha + \gamma_2^\alpha)t^\alpha) > 0,\\
C_R(t) &= C_R(0)E_\alpha(-(\gamma^\alpha + \psi_3^\alpha)t^\alpha) > 0,
\end{aligned}
$$

demonstrating that the axes remain non-negative. Therefore the solution to the model (1) is positive in the $C_V - C_E - C_{IW} - C_{I\overline{W}} - C_R$ plane, consider $t^\star > 0$ then $C_S(t^\star) = 0, C_V(t^\star) > 0, C_E(t^\star) > 0, C_{IW}(t^\star) > 0, C_{I\overline{W}}(t^\star) > 0, C_R(t^\star) > 0$ and $C_S(t) < C_S(t^\star)$. On this plane,

$$D_t^\alpha C_S(t)|_{t=t^\star} = \Lambda^\alpha > 0. \tag{6}$$

By Caputo fractional mean value theorem, it holds $C_S(t) - C_S(t^\star) = \frac{1}{\Gamma(\alpha)} D_t^\alpha(\tau)(t - t^\star)^\alpha,\ \tau \in [t^\star, t)$. As a result, by utilizing Eq. (6), we derive the inequality $C_S(t) > C_S(t^\star)$, which contradicts our initial assumption for $t^\star$. Therefore, any solution $C_S(t)$ is non-negative for all $t \geq 0$. The same approach can be applied to the remaining variables, leading to the conclusion that the solution $\Theta(t)$ remains positive for all $t \geq 0$. To address boundedness, we follow a similar procedure to the integer order case mentioned in Theorem 2.2 of [24] and obtain the expression $N(t) = C_{N_0}E_\alpha(-\gamma^\alpha t^\alpha) + \frac{\Lambda^\alpha}{\gamma^\alpha}(1 - E_\alpha(-\gamma^\alpha t^\alpha))$. This, in turn, implies that the lim sup as $t$ approaches infinity for $N(t)$ is less than or equal to $\frac{\Lambda^\alpha}{\gamma^\alpha}$. □

## 4. Equilibria and the reproduction number

In this section, we will delineate the essential traits of the model before proceeding to determine its mathematical output through a stability analysis. Our focus will be on the equilibrium state where there is an absence of disease, denoted as the "disease-free equilibrium" (DFE) within model (1), symbolized as $\mathscr{D}_1$, and its computation is as follows:

$$
\begin{aligned}
\mathscr{D}_1 &= \left(C_{S0}, C_{V0}, C_{E0}, C_{IW0}, C_{I\overline{W}0}, C_{R0}\right)\\
&= \left(\frac{\Lambda^\alpha(\lambda_3^\alpha + \gamma^\alpha)}{(\gamma^\alpha + \lambda_2^\alpha)(\gamma^\alpha + \lambda_3^\alpha) - \lambda_3^\alpha\lambda_2^\alpha}, \frac{\lambda_2^\alpha\Lambda^\alpha}{(\gamma^\alpha + \lambda_3^\alpha)(\gamma^\alpha + \lambda_2^\alpha) - \lambda_3^\alpha\lambda_2^\alpha}, 0, 0, 0, 0\right).
\end{aligned}
$$

The fundamental determinant in the field of mathematical epidemiology that governs the potential spread or containment of a disease is the basic reproduction number. As a result, in our model (1), we represent the basic reproduction number as $\mathcal{R}_1$, following the approach outlined in Ref. [27]. We have access to the matrices described in [27],

$$
\mathscr{F} = \begin{pmatrix}
0 & \frac{\lambda_1^\alpha\Lambda^\alpha\left[(\gamma^\alpha + \lambda_3^\alpha) + (1-\theta)\lambda_2^\alpha\right]}{(\gamma^\alpha + \lambda_2^\alpha)(\gamma^\alpha + \lambda_3^\alpha) - \lambda_3^\alpha\lambda_2^\alpha} & \frac{\lambda_1^\alpha\eta^\alpha\Lambda^\alpha\left[(\gamma^\alpha + \lambda_3^\alpha) + (1-\theta)\lambda_2^\alpha\right]}{(\gamma^\alpha + \lambda_2^\alpha)(\gamma^\alpha + \lambda_3^\alpha) - \lambda_3^\alpha\lambda_2^\alpha}\\
0 & 0 & 0\\
0 & 0 & 0
\end{pmatrix},
$$

$$
\mathscr{V} = \begin{pmatrix}
(\lambda_4^\alpha + \gamma^\alpha + \mu^\alpha) & 0 & 0\\
-\vartheta\lambda_4^\alpha & (\psi_1^\alpha + \gamma^\alpha + \gamma_1^\alpha) & 0\\
-(1-\vartheta)\lambda_4^\alpha & 0 & (\psi_2^\alpha + \gamma^\alpha + \gamma_2^\alpha)
\end{pmatrix}.
$$

In conclusion, the fundamental representation for model (1) is obtained by examining the spectral radius of the matrix $\rho(\mathscr{F}\mathscr{V}^{-1})$,

$$
\begin{aligned}
\mathcal{R}_1 =& \left[\frac{\lambda_1^\alpha\Lambda^\alpha\vartheta\lambda_4^\alpha\left[(\gamma^\alpha + \lambda_3^\alpha) + (1-\theta)\lambda_2^\alpha\right]}{((\gamma^\alpha + \lambda_2^\alpha)(\gamma^\alpha + \lambda_3^\alpha) - \lambda_3^\alpha\lambda_2^\alpha)(\psi_1^\alpha + \gamma^\alpha + \gamma_1^\alpha)(\lambda_4^\alpha + \gamma^\alpha + \mu^\alpha)}\right]\\
&+ \left[\frac{\lambda_1^\alpha\eta^\alpha\Lambda^\alpha(1-\vartheta)\lambda_4^\alpha\left[(\gamma^\alpha + \lambda_3^\alpha) + (1-\theta)\lambda_2^\alpha\right]}{((\gamma^\alpha + \lambda_2^\alpha)(\gamma^\alpha + \lambda_3^\alpha) - \lambda_3^\alpha\lambda_2^\alpha)(\psi_1^\alpha + \gamma^\alpha + \gamma_2^\alpha)(\lambda_4^\alpha + \gamma^\alpha + \mu^\alpha)}\right],\\
=& \mathcal{R}_{11} + \mathcal{R}_{12},
\end{aligned}
$$

where,

$$
\begin{aligned}
\mathcal{R}_{11} &= \left[\frac{\lambda_1^\alpha\Lambda^\alpha\vartheta\lambda_4^\alpha\left[(\gamma^\alpha + \lambda_3^\alpha) + (1-\theta)\lambda_2^\alpha\right]}{((\gamma^\alpha + \lambda_2^\alpha)(\gamma^\alpha + \lambda_3^\alpha) - \lambda_3^\alpha\lambda_2^\alpha)(\psi_1^\alpha + \gamma^\alpha + \gamma_1^\alpha)(\lambda_4^\alpha + \gamma^\alpha + \mu^\alpha)}\right],\\
\mathcal{R}_{12} &= \left[\frac{\lambda_1^\alpha\eta^\alpha\Lambda^\alpha(1-\vartheta)\lambda_4^\alpha\left[(\gamma^\alpha + \lambda_3^\alpha) + (1-\theta)\lambda_2^\alpha\right]}{((\gamma^\alpha + \lambda_2^\alpha)(\gamma^\alpha + \lambda_3^\alpha) - \lambda_3^\alpha\lambda_2^\alpha)(\psi_1^\alpha + \gamma^\alpha + \gamma_2^\alpha)(\lambda_4^\alpha + \gamma^\alpha + \mu^\alpha)}\right].
\end{aligned}
$$

If the infection continues to exist within the population ((i.e.,), all $C_S, C_V, C_E, C_{IW}, C_{I\overline{W}}, C_R$ greater that or equal to zero), the model has an equilibrium point called endemic equilibrium point, denoted by $\mathscr{D}_1^\star$.

That is, $\left(C_S^\star, C_V^\star, C_E^\star, C_{IW}^\star, C_{I\overline{W}}^\star, C_{R_1}^\star\right) \neq 0$. Then we obtain

$$
\begin{aligned}
&C_S^\star = \frac{k_8 - k_4k_7C_E^\star}{k_6 + k_7C_E^\star},\ C_V^\star = \frac{\lambda_2^\alpha k_4}{k_6 + k_7C_E^\star},\ C_{IW}^\star = k_1C_E^\star,\\
&C_{I\overline{W}}^\star = k_2C_E^\star,\ C_R^\star = k_3C_E,
\end{aligned}
$$

where,

$$
\begin{aligned}
k_1 &= \frac{\vartheta\lambda_4^\alpha}{(\psi_1^\alpha + \gamma^\alpha + \gamma_1^\alpha)},\ k_2 = \frac{(1-\vartheta)\lambda_4^\alpha}{(\psi_2^\alpha + \gamma^\alpha + \gamma_2^\alpha)},\\
k_3 &= \frac{\psi_1^\alpha k_1^\alpha + \psi_2^\alpha k_2^\alpha}{\psi_3^\alpha + \gamma^\alpha},\ k_4 = \frac{(\lambda_4^\alpha + \gamma^\alpha + \mu^\alpha)}{\lambda_1^\alpha(k_1 + \eta^\alpha k_2)},\\
k_5 &= \frac{((1-\theta)\lambda_1^\alpha k_1 + (1-\theta)\lambda_1^\alpha\eta^\alpha k_2)}{\lambda_1^\alpha(k_1 + \eta^\alpha k_2)},\ k_6 = k_5 + (\lambda_3^\alpha + \gamma^\alpha),\\
k_7 &= (1-\theta)\lambda_1^\alpha k_1 + (1-\theta)\lambda_1^\alpha\eta^\alpha k_2,\\
k_8 &= k_4k_6 - k_5\lambda_2^\alpha k_4,
\end{aligned}
$$

and $C_E^\star$ is the positive root of the equation $P_1C_{E_1}^2 + P_2C_{E_1} + P_3 = 0$.

Here,

$$
\begin{aligned}
P_1 &= \lambda_1^\alpha k_1k_4k_7 + \eta^\alpha k_2k_4k_7 + \mu^\alpha k_7 + \psi_3^\alpha k_3k_7,\\
P_2 &= \Lambda^\alpha k_7 - \lambda_1^\alpha k_1k_8 - \eta^\alpha k_2k_8 - (\gamma^\alpha + \lambda_2^\alpha)k_4k_7 + \mu^\alpha k_6 + \psi_3^\alpha k_3k_6,\\
P_3 &= \Lambda^\alpha k_6 - (\gamma^\alpha + \lambda_2^\alpha)k_8 + \lambda_3^\alpha\lambda_2^\alpha k_4 + \mu^\alpha k_6.
\end{aligned}
$$

## 5. Global stability of an equilibria

In this section, we will show the global stability by Lyapunov stability theory [28] and LaSalle's invariance principle [29].

To show the global stability of $\mathscr{D}_1$, we assume the following condition

$$\left(1 - \frac{C_SC_{V0}}{C_{S0}C_V}\right) \leq 0,\ \forall\ C_S \geq 0,\ C_V \geq 0\ \ (C_0) \tag{7}$$

**Theorem 5.1.** *The equilibrium point $\mathscr{D}_1$ is globally asymptotically stable if $\mathcal{R}_1 \leq 0$.*

**Proof.** Let the following Lyapunov function $L_0$

$$
\begin{aligned}
L_0 =& C_{S0}\left(\frac{C_S}{C_{S0}} - \ln\left(\frac{C_S}{C_{S0}}\right) - 1\right) + C_{V0}\left(\frac{C_V}{C_{V0}} - \ln\left(\frac{C_V}{C_{V0}}\right) - 1\right)\\
&+ C_E + C_{IW} + C_{I\overline{W}} + C_R
\end{aligned} \tag{8}
$$

The $\alpha$ derivative of $L_0$ is given by

$$
\begin{aligned}
D^\alpha L_0 \leq& \left(1 - \frac{C_{S0}}{C_S}\right)D^\alpha C_S + \left(1 - \frac{C_{V0}}{C_V}\right)D^\alpha C_V + D^\alpha C_E + D^\alpha C_IW\\
&+ D^\alpha C_{I\overline{W}} + D^\alpha C_R\\
\leq& \Lambda^\alpha - \gamma^\alpha C_S\gamma^\alpha C_V - \gamma^\alpha C_E - \gamma^\alpha C_{IW} - \gamma^\alpha C_{I\overline{W}} - \gamma^\alpha C_R\\
&- \frac{C_S0}{CS}\Lambda^\alpha + \lambda_1^\alpha C_{S0}C_{IW}
\end{aligned} \tag{9}
$$

$$+ \lambda_1^\alpha \eta^\alpha C_{S0} C_{I\overline{W}} - \lambda_3^\alpha C_V \frac{C_{S0}}{C_S} - \mu^\alpha C_E \frac{C_{S0}}{C_S} + \gamma^\alpha C_{S0}$$
$$- \psi_3^\alpha C_R \frac{C_{S0}}{C_S} - \lambda_2^\alpha C_S \frac{C_{V0}}{C_V}$$
$$- (1-\theta)\lambda_1^\alpha C_{IW} C_{V0} + \lambda_1^\alpha \eta^\alpha C_{I\overline{W}} C_{V0} + \lambda_2^\alpha C_{S0} \tag{10}$$
$$\leq \Lambda^\alpha \left(2 - \frac{C_{S0}}{C_S} - \frac{C_S}{C_{S0}}\right) + \lambda_2^\alpha C_{S0} \left(1 - \frac{C_S C_{V0}}{C_{S0} C_V}\right)$$
$$+ \gamma^\alpha \left(C_{IW} + C_{I\overline{W}}\right)\left(R_0 - 1\right). \tag{11}$$

Because the arithmetic mean is either greater than or equal to the geometric mean,

$$\left(2 - \frac{C_{S0}}{C_S} - \frac{C_S}{C_{S0}}\right) \leq 0. \tag{12}$$

As this equilibrium point checks the condition $C_0$, then we will have

$$\left(1 - \frac{C_S C_{V0}}{C_{S0} C_V}\right) \leq 0. \tag{13}$$

Finally, if $R_0 \leq 1$, then $D^\alpha L_0 \leq 0$. Let us define $B_0 = \{(C_S, C_V, C_E, C_{IW}, C_{I\overline{W}}, C_R) \mid D^\alpha L_0 = 0\}$, then the greatest subset positively invariant of $B_0$ is given by the singleton $\mathscr{D}_1$. By using the LaSalle's invariance principle, we conclude that the equilibrium point $\mathscr{D}_1$ is globally asymptotically stable. □

## 6. Numerical interpretation and analysis

In this section, we present a comprehensive analysis of numerical findings regarding the fractional chickenpox model, drawing meaningful comparisons with outcomes obtained from the classical chicken model as studied by Sayooj et al. [24]. To address the system (1), we employ the adaptive predictor–corrector algorithm as outlined in [30]. By leveraging this methodology, we can efficiently compute approximations for various essential variables, including $C_{Sk}$, $C_{Vk}$, $C_{Ek}$, $C_{IWk}$, $C_{I\overline{W}k}$, and $C_{Rk}$, while considering the constraints of $N \in \mathbb{N}$ and $T > 0$. These iterative formulas not only facilitate a deeper understanding of the fractional chickenpox model but also enable insightful comparisons with the classical chicken model's results.

$$C_{Sk} \approx C_{S0} + \frac{\rho^\alpha h^\alpha}{\Gamma(\alpha+2)} \sum_{l=0}^{k} a_{l,k+1} \{\Lambda^\alpha - \lambda_1^\alpha C_{Sl}(C_{IWl} + \eta^\alpha C_{I\overline{W}l}) + \lambda_3^\alpha C_{Vl} + \mu^\alpha C_{El} - (\gamma^\alpha + \lambda_2^\alpha) C_{Sl} + \psi_3^\alpha C_{Rl}\} + \frac{\rho^\alpha h^\alpha}{\Gamma(\alpha+2)} \{\Lambda^\alpha - \lambda_1^\alpha C_S^p{}_{k+1}(C_{IW}^p{}_{k+1} + \eta^\alpha C_{I\overline{W}}^p{}_{k+1}) + \lambda_3^\alpha C_V^p{}_{k+1} + \mu^\alpha C_E^p{}_{k+1} - (\gamma^\alpha + \lambda_2^\alpha) C_S^p{}_{k+1} + \psi_3^\alpha C_R^p{}_{k+1}\},$$

$$C_{Vk+1} \approx C_{V0} = \frac{\rho^\alpha h^\alpha}{\Gamma(\alpha+2)} \sum_{l=0}^{k} a_{l,k+1} \{\lambda_2^\alpha C_{Sl} - (1-\theta)\lambda_1^\alpha C_{IWl} C_{Vl} - (1-\theta)\lambda_1^\alpha \eta^\alpha C_{I\overline{W}l} C_{Vl} - (\lambda_3^\alpha \gamma^\alpha) \times C_{Vl}\} + \frac{\rho^\alpha h^\alpha}{\Gamma(\alpha+2)} \{\lambda_2^\alpha C_S^p{}_{k+1} - (1-\theta)\lambda_1^\alpha C_{IW}^p{}_{k+1} C_V^p{}_{k+1} - (1-\theta)\lambda_1^\alpha \eta^\alpha C_{I\overline{W}}^p{}_{k+1} C_V^p{}_{k+1} - (\lambda_3^\alpha + \gamma^\alpha) C_V^p{}_{k+1}\},$$

$$C_{Ek+1} \approx C_{E0} + \frac{\rho^\alpha h^\alpha}{\Gamma(\alpha+2)} \sum_{l=0}^{k} a_{l,k+1} \{(1-\theta)\lambda_1^\alpha C_{IWl} C_{Vl} + (1-\theta)\lambda_1^\alpha \eta^\alpha C_{I\overline{W}l} C_{Vl} + \lambda_1^\alpha C_{Sl}(C_{IWl} + \eta^\alpha C_{I\overline{W}l}) - (\lambda_4^\alpha + \gamma^\alpha + \mu^\alpha) C_{El}\} + \frac{\rho^\alpha h^\alpha}{\Gamma(\alpha+2)} \{(1-\theta)\lambda_1^\alpha C_{IW}^p{}_{k+1} C_V^p{}_{k+1} + (1-\theta)\lambda_1^\alpha \eta^\alpha C_{I\overline{W}}^p{}_{k+1} \times C_V^p{}_{k+1} + \lambda_1^\alpha C_S^p{}_{k+1}(C_{IW}^p{}_{k+1} + \eta^\alpha C_{I\overline{W}}^p{}_{k+1}) - (\lambda_4^\alpha + \gamma^\alpha + \mu^\alpha) C_E^p{}_{k+1}\},$$

$$C_{IWk+1} \approx C_{IW0} + \frac{\rho^\alpha h^\alpha}{\Gamma(\alpha+2)} \sum_{l=0}^{k} a_{l,k+1} \{(1-\vartheta)\lambda_4^\alpha C_{El} - (\psi_2^\alpha + \gamma^\alpha + \gamma_2^\alpha) C_{I\overline{W}l}\} + \frac{\rho^\alpha h^\alpha}{\Gamma(\alpha+2)} \{\vartheta \lambda_4^\alpha C_E^p{}_{k+1} - (\psi_1^\alpha + \gamma^\alpha + \gamma_1^\alpha) C_{IW}^p{}_{k+1}\},$$

$$C_{I\overline{W}k+1} \approx C_{I\overline{W}0} + \frac{\rho^\alpha h^\alpha}{\Gamma(\alpha+2)} \sum_{l=0}^{k} a_{l,k+1} \{(1-\vartheta)\lambda_4^\alpha C_{El} - (\psi_2^\alpha + \gamma^\alpha + \gamma_2^\alpha) C_{I\overline{W}l}\} + \frac{\rho^\alpha h^\alpha}{\Gamma(\alpha+2)} \{(1-\vartheta)\lambda_4^\alpha C_E^p{}_{k+1} - (\psi_2^\alpha + \gamma^\alpha + \gamma_2^\alpha) C_{I\overline{W}}^p{}_{k+1}\},$$

$$C_{Rk+1} \approx C_{R0} + \frac{\rho^\alpha h^\alpha}{\Gamma(\alpha+2)} \sum_{l=0}^{k} a_{l,k+1} \{\psi_1^\alpha C_{IWl} + \psi_2^\alpha C_{I\overline{W}l} - (\gamma^\alpha + \psi_3^\alpha) C_{Rl}\} + \frac{\rho^\alpha h^\alpha}{\Gamma(\alpha+2)} \{\psi_1^\alpha C_{IW}^p{}_{k+1} + \psi_2^\alpha \times C_{I\overline{W}}^p{}_{k+1} - (\gamma^\alpha + \psi_3^\alpha) C_R^p{}_{k+1}\}.$$

where $h = \frac{T^\rho}{N}$ and

$$C_{Sk} \approx C_{S0} + \frac{\rho^\alpha h^\alpha}{\Gamma(\alpha+2)} \left((k+1-l)^{\alpha-(k-l)^\alpha}\right) \{\Lambda^\alpha - \lambda_1^\alpha C_{Sl}(C_{IWl} + \eta^\alpha C_{I\overline{W}l}) + \lambda_3^\alpha C_{Vl} + \mu^\alpha C_{El} - (\gamma^\alpha + \lambda_2^\alpha) C_{Sl} + \psi_3^\alpha C_{Rl}\},$$

$$C_{Vk+1} \approx C_{V0} = \frac{\rho^\alpha h^\alpha}{\Gamma(\alpha+2)} \left((k+1-l)^{\alpha-(k-l)^\alpha}\right) \{\lambda_2^\alpha C_{Sl} - (1-\theta)\lambda_1^\alpha C_{IWl} C_{Vl} - (1-\theta)\lambda_1^\alpha \eta^\alpha C_{I\overline{W}l} \times C_{Vl} - (\lambda_3^\alpha \gamma^\alpha) C_{Vl}\},$$

$$C_{Ek+1} \approx C_{E0} + \frac{\rho^\alpha h^\alpha}{\Gamma(\alpha+2)} \left((k+1-l)^{\alpha-(k-l)^\alpha}\right) \{(1-\theta)\lambda_1^\alpha \times C_{IWl} C_{Vl} + (1-\theta)\lambda_1^\alpha \eta^\alpha C_{I\overline{W}l} C_{Vl} + \lambda_1^\alpha C_{Sl}(C_{IWl} + \eta^\alpha C_{I\overline{W}l}) - (\lambda_4^\alpha + \gamma^\alpha + \mu^\alpha) C_{El}\},$$

$$C_{IWk+1} \approx C_{IW0} + \frac{\rho^\alpha h^\alpha}{\Gamma(\alpha+2)} \left((k+1-l)^{\alpha-(k-l)^\alpha}\right) \{(1-\vartheta)\lambda_4^\alpha C_{El} - (\psi_2^\alpha + \gamma^\alpha + \gamma_2^\alpha) C_{I\overline{W}l}\},$$

$$C_{I\overline{W}k+1} \approx C_{I\overline{W}0} + \frac{\rho^\alpha h^\alpha}{\Gamma(\alpha+2)} \left((k+1-l)^{\alpha-(k-l)^\alpha}\right) \{(1-\vartheta)\lambda_4^\alpha C_{El} - (\psi_2^\alpha + \gamma^\alpha + \gamma_2^\alpha) C_{I\overline{W}l}\},$$

$$C_{Rk+1} \approx C_{R0} + \frac{\rho^\alpha h^\alpha}{\Gamma(\alpha+2)} \left((k+1-l)^{\alpha-(k-l)^\alpha}\right) \{\psi_1^\alpha C_{IWl} + \psi_2^\alpha C_{I\overline{W}l} - (\gamma^\alpha + \psi_3^\alpha) C_{Rl}\}.$$

To validate the outcomes of our analytical experiments, we have conducted numerical experiments to corroborate our findings. In these experiments, we focus on the population of Phuket in the year 2021, which amounted to 418,785 individuals. Phuket Province, located in Thailand, comprises three distinct districts: Kathu, Mueang Phuket, and Thalang. Remarkably, Mueang Phuket District has recorded more than 300 cases of chickenpox, as documented in the comprehensive study by Sayooj [24]. Conversely, Thalang District reports fewer than 300 chickenpox cases, offering valuable insights into the geographical variation of this disease's prevalence within Phuket. For our numerical experiments, we have utilized data from a deterministic model, and the initial population figures are as follows: Susceptible individuals amount to 83,812, with 573 individuals having been vaccinated, 604 individuals in the exposed stage, and 70 individuals facing infections with complications. Moreover, there are 464 individuals dealing with uncomplicated infections, while 178 individuals have successfully recovered from chickenpox. By incorporating this data into our numerical investigations, we aim to provide a more comprehensive understanding

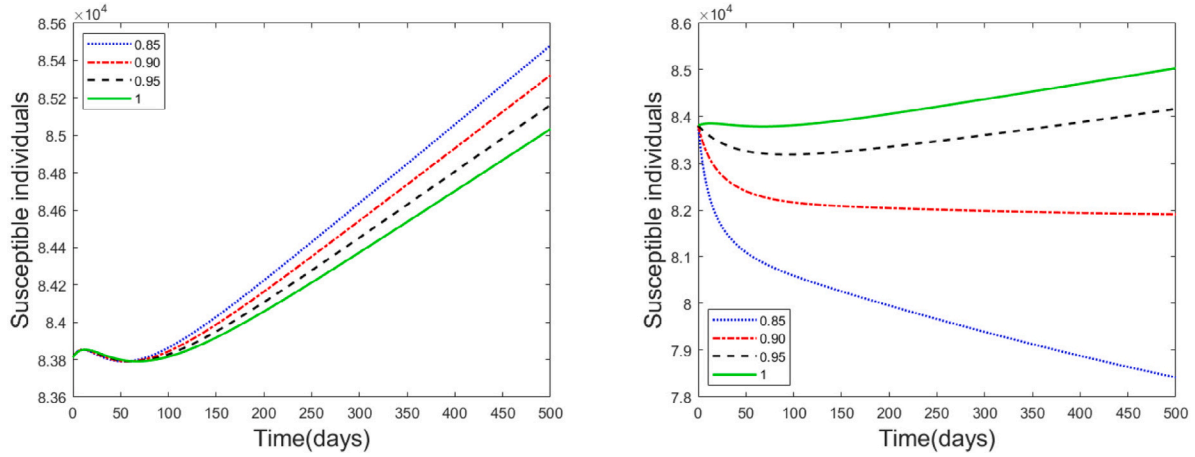


**Fig. 1.** (a) The model simulations for the susceptible class are carried out with different fractional-order values of $\alpha$, without exponentiating the parameters (b) The model simulation for the susceptible class involves various fractional-order $\alpha$ values, and the parameters are raised to the power of $\alpha$.

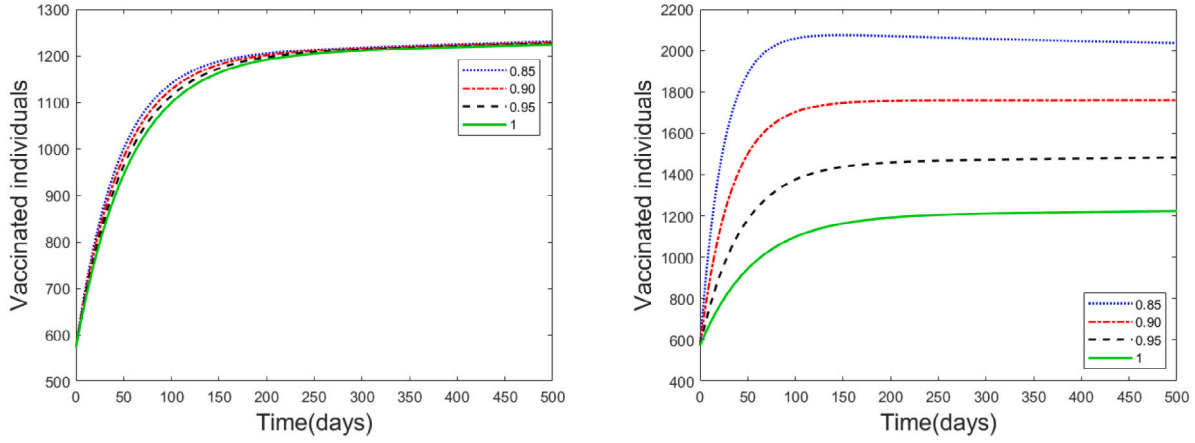


**Fig. 2.** (a) The model simulations for the vaccinated class are carried out with different fractional-order values of $\alpha$, without exponentiating the parameters (b) The model simulation for the vaccinated class involves various fractional-order $\alpha$ values, and the parameters are raised to the power of $\alpha$.

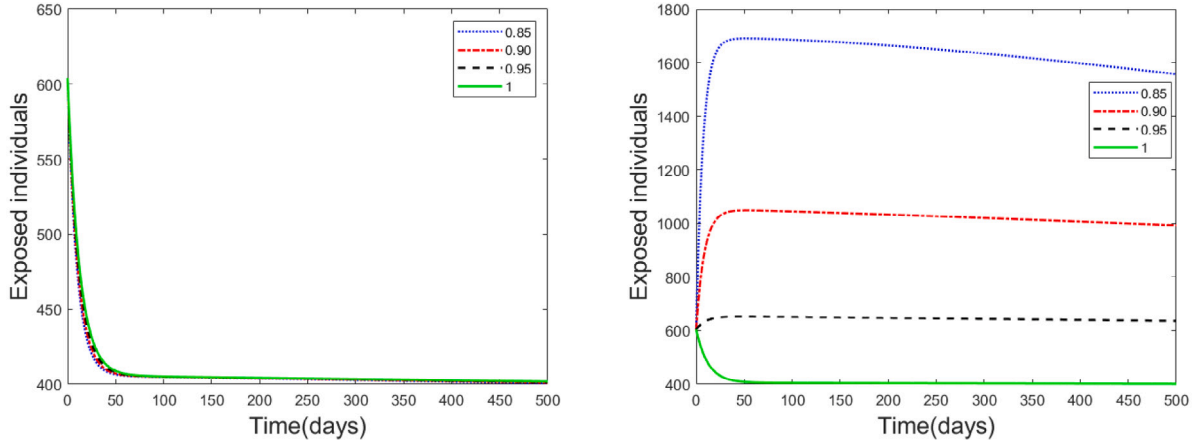


**Fig. 3.** (a) The model simulations for the exposed class are carried out with different fractional-order values of $\alpha$, without exponentiating the parameters (b) The model simulation for the exposed class involves various fractional-order $\alpha$ values, and the parameters are raised to the power of $\alpha$.

of the chickenpox dynamics in Phuket and shed light on potential strategies for disease management in the region.

To grasp the proposed concept of parameter exponentiation, we conducted numerical simulations using field data on chickenpox in Phuket, Thailand. All model parameters were configured according to the values specified in Table 1. In Figs. 1(a) to 6(a), we illustrate the temporal evolution of the susceptible, vaccinated, infected (with and without complications), and recovered populations without applying parameter exponentiation. When comparing Figs. 1(a) to 1(b), we observe that the susceptible population exhibits exponential decay when parameter exponentiation is introduced. Crucially, when we exponentiate the parameters with the fractional order $\alpha$, there is a notable

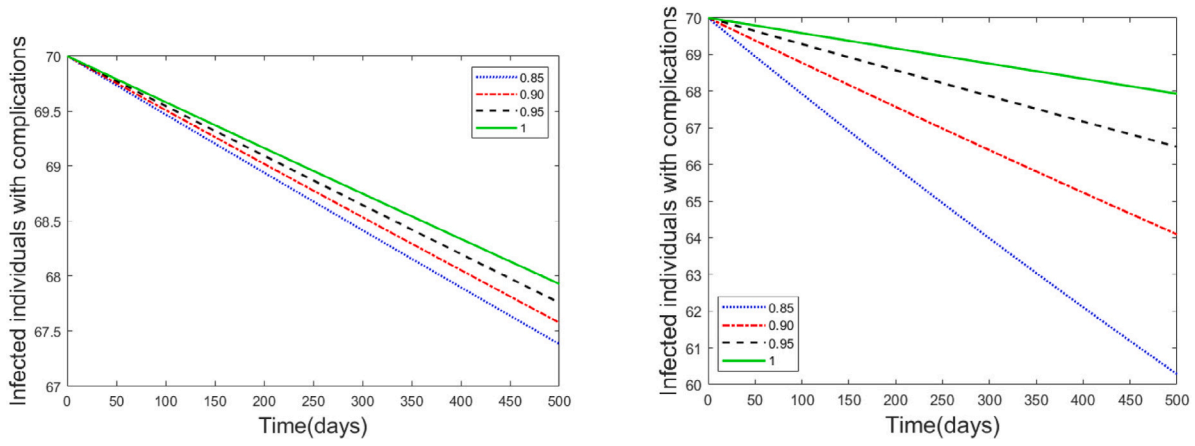


**Fig. 4.** (a) The model simulations for the infected individuals with complications class are carried out with different fractional-order values of $\alpha$, without exponentiating the parameters (b) The model simulation for the infected individuals with complications class involves various fractional-order $\alpha$ values, and the parameters are raised to the power of $\alpha$.

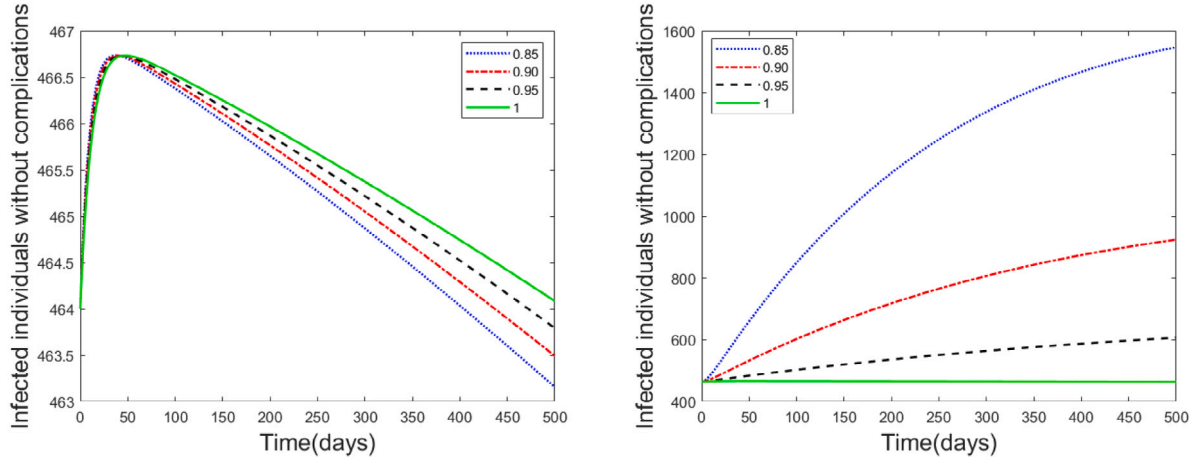


**Fig. 5.** (a) The model simulations for the infected individuals without complications class are carried out with different fractional-order values of $\alpha$, without exponentiating the parameters (b) The model simulation for the infected individuals without complications class involves various fractional-order $\alpha$ values, and the parameters are raised to the power of $\alpha$.

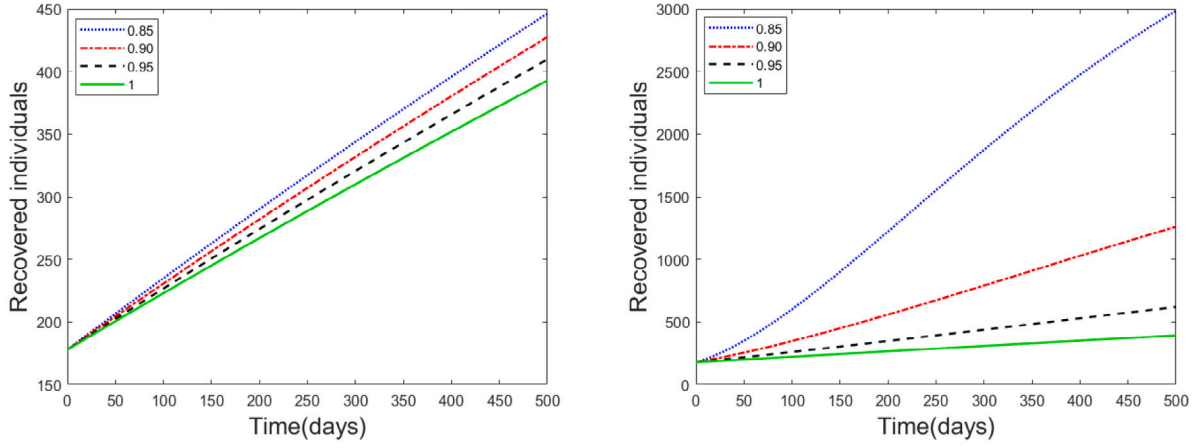


**Fig. 6.** (a) The model simulations for the recovered class are carried out with different fractional-order values of $\alpha$, without exponentiating the parameters (b) The model simulation for the recovered class involves various fractional-order $\alpha$ values, and the parameters are raised to the power of $\alpha$.

and rapid upsurge in the rate of vaccination within the population, as visually depicted in Fig. 2(b). This contrasts sharply with the scenario where parameters are left unexponentiated, as evident in Fig. 2(a). The effect of parameter exponentiation on the rate of vaccination becomes particularly striking, underlining the significant impact of this approach on the dynamics of vaccination within the model. In Fig. 3(a), the variation in the exposed class is depicted without exponentiating the powers of the parameters. In Fig. 3(b), on the other hand, the

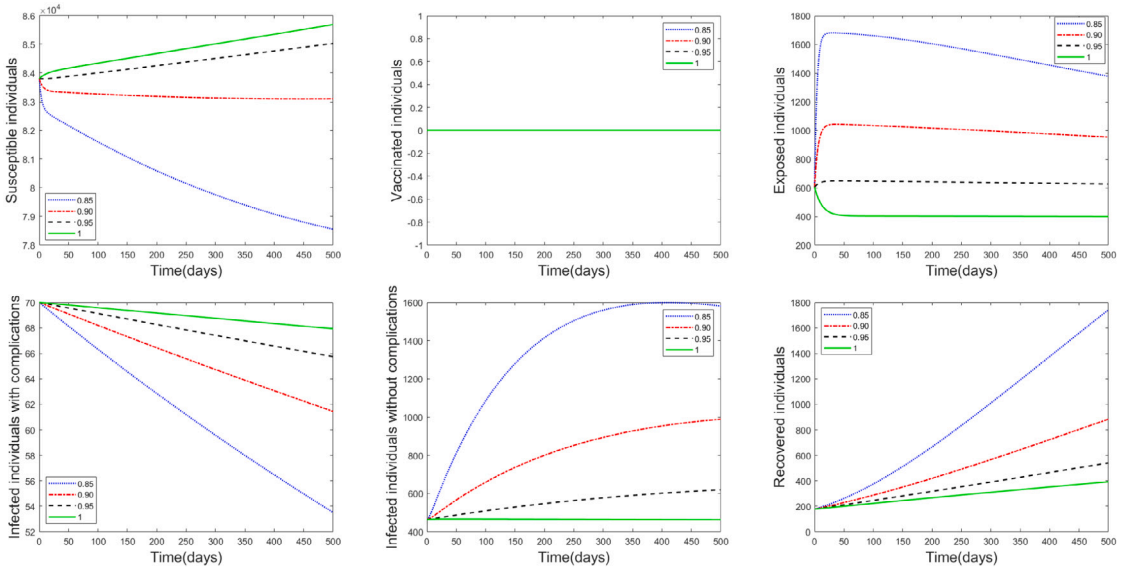


**Fig. 7.** The impact of vaccination and the notable decrease in recovered population in the absence of vaccination is presented for various values of $\alpha$.

change in the exposed class is shown after exponentiating the powers of the parameters. The infected population is divided into two distinct compartments, namely those with complications and those without complications. In both of these compartments, a marked and swift decline in the number of infected individuals is evident when the model parameters are elevated to the power of the fractional order $\alpha$, as demonstrated in both Figs. 4 and 5. Furthermore, a similar trend can be observed in the recovered population, where there is a noticeable increase when the exponentiated model is considered. This highlights the compelling influence of applying parameter exponentiation on the dynamics of both infected and recovered populations within the model.

## 7. Influence of vaccination

In this section, we delve into the profound impact of vaccination on mitigating the prevalence of chickenpox in Thailand. The pivotal role played by vaccination becomes evident when considering a time frame of 500 days. During this period, the population of susceptible individuals experiences a notable decline due to the protective effects of vaccination. As a result, the number of exposed individuals, both with and without complications, shows a discernible increase. This rise is indicative of the broader coverage and efficacy of the vaccination strategy. Moreover, the vaccination campaign contributes significantly to the escalation in the count of individuals with complications, highlighting the effectiveness of immunization in preventing severe cases. Simultaneously, the population of recovered individuals gradually decreases as the incidence of new cases diminishes. This intricate dance between susceptibility, exposure, and recovery underscores the dynamic influence of vaccination in shaping the epidemiological landscape of chickenpox in Thailand. These insights affirm the instrumental role played by vaccination programs in fostering public health and curtailing the impact of infectious diseases.

By comparing the figures Figs. 1–6 with Fig. 7, we can observe that the recovery rate of infected individuals are higher while we incoporate the vaccination strategy with parameter exponentiation (Ref. Table 2). While analyzing, the mathematical model with parameter exponentiation that considers effective vaccination we observed drastic increase in the recovered population.

The impact of considering precautionary measures is depicted in Fig. 8. In that numerical simulation we get that, for the values of $\alpha = 0.4$ and $\mu = 0.06$ the basic reproduction number takes the values less than one. Similarly, $R_1 < 1$ when for $\alpha = 0.6$ and $\mu = 0.08$, $\alpha = 0.8$ and $\mu = 0.09$, and $\alpha = 1$ and $\mu = 0.1$. That is for the values of $\mu \leq 0.1$, our proposed model is locally stable.

Table 3 provides a statistical summary of $\mathcal{R}_1$, offering insights into its characteristics across different values of $\alpha$ such as $0.4, 0.6, 0.8$ and $1$. The data for $\mathcal{R}_1$ is extracted from Fig. 8. This table allows us to delve deeper into the behavior of $\mathcal{R}_1$ at varying alpha levels. It furnishes a comprehensive perspective on $\mathcal{R}_1$, encompassing key parameters such as maximum, minimum, mean, median, standard deviation, and range. In doing so, it illuminates the variability and trends exhibited by $\mathcal{R}_1$ under distinct $\alpha$ conditions.

In Fig. 9, we gain insights into how changes in the control parameters $\mu$, ranging from 0 to 5, and $\lambda_1$, varying between 0 and $5 \times 10^{-6}$, impact the stability of the proposed Chickenpox model in Phuket province, Thailand. This investigation is conducted for different fractional orders $\alpha$, and it reveals variations in the reproduction number $\mathcal{R}_1$. Fig. 9 assists us in identifying specific combinations of $\mu$ and $\lambda_1$ values where the basic reproduction number falls below one, signifying a significant reduction in disease transmission.

## 8. Conclusion

In summary, this paper presented a fractional order model for the spread of Chickenpox in Phuket Province, encompassing six distinct compartments representing the susceptible, vaccinated, exposed, infected individuals with complications, and infected individuals without complications. We established crucial theorems concerning the existence, uniqueness, and boundedness of all model variables. Furthermore, we identified two equilibrium points: the disease-free steady state and the endemic equilibrium and calculated the basic reproduction number using next generation matrix methods.

Our analysis revealed that the stability of these equilibrium points depends on the basic reproduction number. Through numerical simulations, we not only validated our theoretical findings but also highlighted the impact of the fractional derivative order on the infection dynamics. The efficacy of the proposed approach is assessed through an examination of various scenarios, including situations before the incorporation of parameter exponentiation in the context of vaccination, after the introduction of parameter exponentiation, and scenarios without vaccination but with parameter exponentiation. Through these analyses, it was noted that the recovery rate of infected individuals exhibited a significant increase in the model that incorporated parameter exponentiation, particularly in the presence of an effective vaccination

**Table 2**
The importance of vaccination at three possible cases at various values of $\alpha$.

| Dynamics of Recovered population | $\alpha = 0.85$ | $\alpha = 0.90$ | $\alpha = 0.95$ | $\alpha = 1.0$ |
|---|---|---|---|---|
| With vaccination without exponentiation of parameters | 445 | 428 | 408 | 380 |
| Without vaccination with exponentiation of parameters | 1725 | 876 | 537 | 389 |
| With vaccination with exponentiation of parameters | 2979 | 1261 | 617 | 395 |

**Table 3**
Statistical Summary of $\mathcal{R}_1$.

| $\alpha$ | Minimu | Maximum | Mean | Median | Mode | Standard deviation | Range |
|---|---|---|---|---|---|---|---|
| 0.4 | 0.1388 | 1.497 | 0.3079 | 0.1779 | 0.1388 | 0.3974 | 1.358 |
| 0.6 | 0.07567 | 2.749 | 0.368 | 0.1131 | 0.07567 | 0.792 | 2.674 |
| 0.8 | 0.04509 | 5.526 | 0.5929 | 0.07803 | 0.04509 | 1.638 | 5.481 |
| 1 | 0.04965 | 20.43 | 1.988 | 0.09907 | 0.04965 | 6.116 | 20.38 |

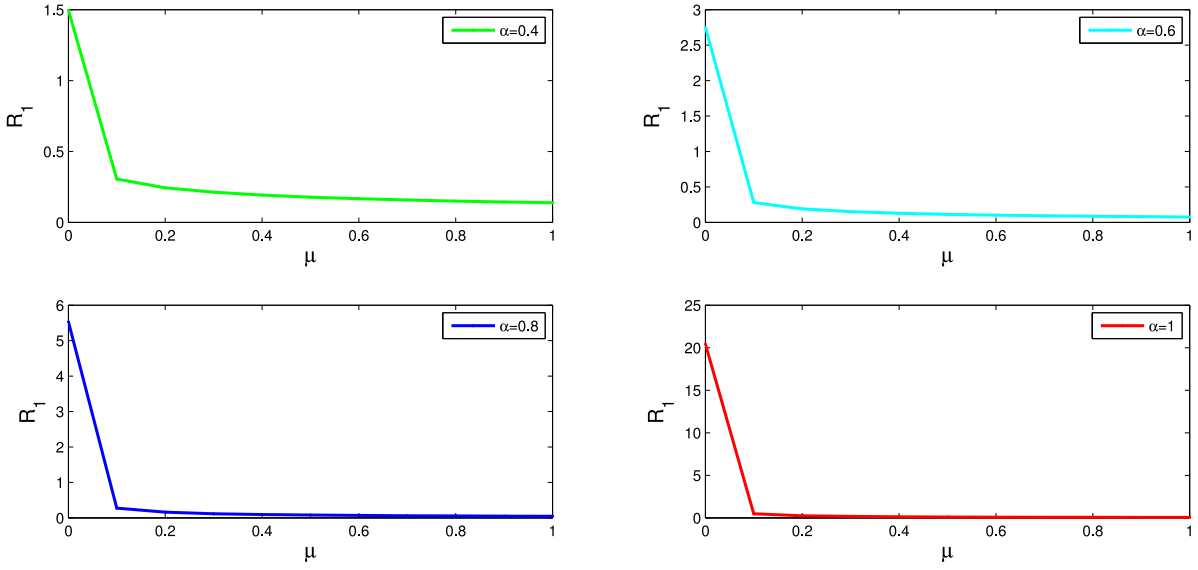


**Fig. 8.** Effect of Precautionary Measures and $\mathcal{R}_1$.

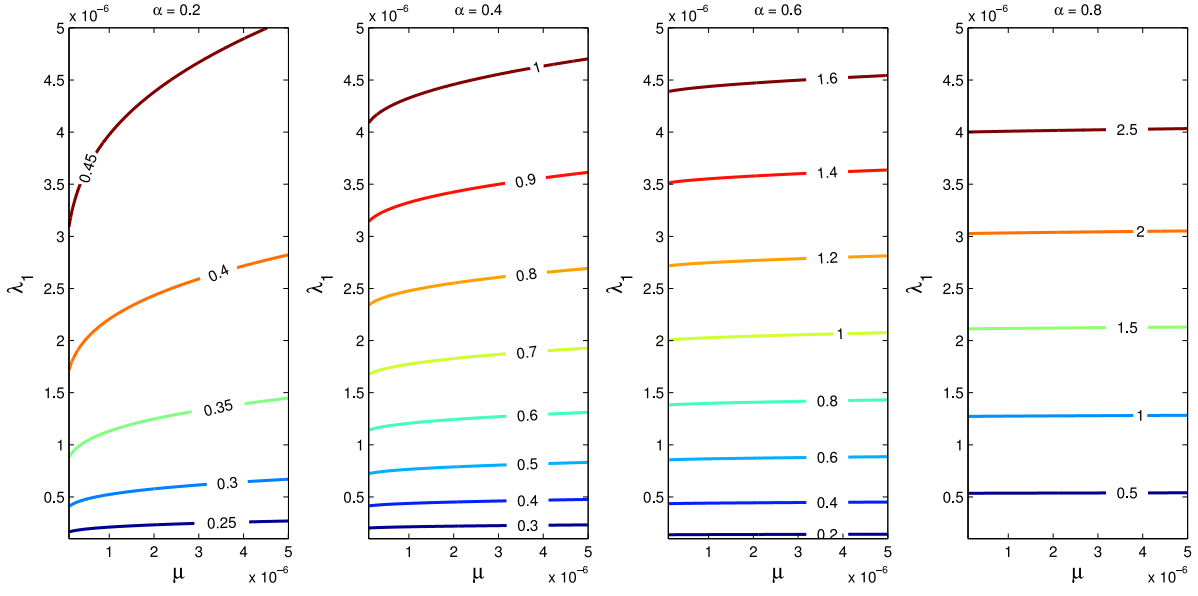


**Fig. 9.** The contour plot of $\mathcal{R}_1$ in terms of $\mu$ and $\lambda_1$ at $\alpha = 0.2, 0.4, 0.6, 0.8$.

strategy. Specifically, we found that the fractional derivative does not affect the stability of the equilibria but significantly influences the rate at which model variables converge to their respective steady states. Notably, higher fractional derivative orders lead to a faster convergence of these variables.

## CRediT authorship contribution statement

**Sayooj Aby Jose:** Conceptualization, Data curation, Formal analysis, Methodology, Resources, Software, Validation, Visualization, Writing – original draft, Writing – review & editing. **Zakaria Yaagoub:** Formal analysis, Methodology, Validation, Resources, Writing – review & editing. **Dianavinnarasi Joseph:** Data curation, Formal analysis, Validation, Visualization, Writing – review & editing, Methodology, Software. **Raja Ramachandran:** Conceptualization, Funding acquisition, Investigation, Supervision, Validation, Writing – review & editing. **Anuwat Jirawattanapanit:** Conceptualization, Funding acquisition, Investigation, Project administration, Supervision, Validation, Writing – review & editing.

## Declaration of competing interest

The authors declare that they have no known competing financial interests or personal relationships that could have appeared to influence the work reported in this paper.

## Data availability

No data was used for the research described in the article.

## Acknowledgments

This article has been written with the joint partial financial support of IMU Breakout Graduate Fellowship Award funded by International Mathematical Union (IMU), Germany with the assistance of Friends of the International Mathematical Union (FIMU), USA (Ref IMU-BGF-2021-07) , RUSA-Phase 2.0 grant sanctioned vide letter No. F 2451/2014-U, Govt. of India, Policy (TN Multi-Gen), Dept. of Edn.Govt. of India, Centre for Nonlinear Systems, Chennai Institute of Technology, India, vide funding number CIT/CNS/2023/RP-017, The researcher expresses deep gratitude for the valuable help extended by the Research and Development Institute. The research fund received substantial support from Phuket Rajabhat University, for which the researcher is greatly appreciative.

## References

[1] M. Almuneef, Z.A. Memish, H.H. Balkhy, B. Alotaibi, M. Helmy, Chickenpox complications in Saudi Arabia: Is it time for routine varicella vaccination? Int. J. Infect. Dis. 10 (2) (2006) 156–161.
[2] A.A. Gershon, Varicella-zoster virus infections, Pediatr. Rev. 29 (1) (2008) 5–11.
[3] L. Gregorakos, P. Myrianthefs, N. Markou, D. Chroni, E. Sakagianni, Severity of illness and outcome in adult patients with primary varicella pneumonia, Respiration 69 (4) (2002) 330–334.
[4] C.K. Fairley, E. Miller, Varicella-zoster virus epidemiology-a changing scene? J. Infect. Dis. 174 (Supplement-3) (1996) S314–S319.
[5] J. Yang, F. Afzal, P. Appiah, Fractional derivative for varicella-zoster virus using two-scale fractal dimension approach with vaccination, Adv. Math. Phys. 2022 (2022) 1725110.
[6] Lee, Review of varicella zoster seroepidemiology in India and South-east Asia, Trop. Med. Int. Health 3 (11) (1998) 886–890.
[7] S.R. Preblud, Varicella: complications and costs, Pediatrics 78 (4) (1986) 728–735.
[8] R. Muench, C. Nassim, S. Niku, J.Z. Sullivan-Bolyai, Seroepidemiology of varicella, J. Infect. Dis. 153 (1) (1986) 153–155.
[9] M. Wharton, The epidemiology of varicella-zoster virus infections, Infect. Dis. Clin. 10 (3) (1996) 571–581.
[10] J.P. Struewing, K.C. Hyams, J.E. Tueller, G.C. Gray, The risk of measles, mumps, and varicella among young adults: a serosurvey of US Navy and Marine Corps recruits, Am J Public Health 83 (12) (1993) 1717–1720.
[11] A. Ghafoor, N. Khan, M. Hussain, R. Ullah, A hybrid collocation method for the computational study of multi-term time fractional partial differential equations, Comput. Math. Appl. 128 (2022) 130–144.
[12] R.L. Magin, Fractional calculus models of complex dynamics in biological tissues, Comput. Math. Appl. 59 (5) (2010) 1586–1593.
[13] N. Anggriani1, H.S. Panigoro, E. Rahmi, O.J. Peter, S.A. Jose, A predator-prey model with additive Allee effect and intraspecific competition on predator involving Atangana-Baleanu-Caputo derivative, Results Phys. 2023 (2023) 106489.
[14] M. El-Shahed, F.A. El-Naby, Fractional calculus model for childhood diseases and vaccines, Appl. Math. Sci. 8 (98) (2014) 4859–4866.
[15] F. Haq, M. Shahzad, S. Muhammad, H.A. Wahab, Numerical analysis of fractional order epidemic model of childhood diseases, Discrete Dyn. Nat. Soc. 2017 (2017) 4057089.
[16] A. Ullah, T. Abdeljawad, S. Ahmad, K. Shah, Study of a fractional-order epidemic model of childhood diseases, J. Funct. Spaces 2020 (2020) 5895310.
[17] J. Dianavinnarasi, R. Raja, J. Alzabut, M. Niezabitowski, O. Bagdasar, Controlling wolbachia transmission and invasion dynamics among aedes aegypti population via impulsive control strategy, Symmetry 13 (3) (2021) 434.
[18] J. Dianavinnarasi, R. Raja, J. Alzabut, J. Cao, M. Niezabitowski, O. Bagdasar, Application of Caputo–Fabrizio operator to suppress the Aedes Aegypti mosquitoes via Wolbachia: An LMI approach, Math. Comput. Simulation 201 (2022) 462–485.
[19] S.A. Jose, R. Raja, B.I. Omede, R.P. Agarwal, J. Alzabut, J. Cao, V.E. Balas, Mathematical modeling on co-infection: Transmission dynamics of zika virus and dengue fever, Nonlinear Dynam. 111 (2023) 4879–4914.
[20] S.A. Jose, R. Raja, D. Baleanu, H.S. Panigoro, V.E. Balas, Computational dynamics of a fractional order substance addictions transfer model with Atangana–Baleanu–Caputo derivative, Math. Methods Appl. Sci. (2022) 1–26.
[21] M. Helikumi, G. Eustace, S. Mushayabasa, Dynamics of a fractional-order chikungunya model with asymptomatic infectious class, Comput. Math. Methods Med. 2022 (2022) 5118382.
[22] H.M. Alshehri, A. Khan, A fractional order Hepatitis C mathematical model with Mittag-Leffler kernel, J. Funct. Spaces 2021 (2021) 1–10.
[23] I. Ameen, M. Hidan, Z. Mostefaoui, H.M. Ali, Fractional optimal control with fish consumption to prevent the risk of coronary heart disease, Complexity 2020 (2020) 1–13.
[24] S.A. Jose, R. Raja, J. Dianavinnarasi, D. Baleanu, A. Jirawattanapanit, Mathematical modeling of chickenpox in Phuket: Efficacy of precautionary measures and bifurcation analysis, Biomed. Signal Process. Control 84 (2023) 104714.
[25] K. Diethelm, A fractional calculus based model for the simulation of an outbreak of dengue fever, Nonlinear Dynam. 71 (2013) 613–619.
[26] T.A. Biala, A.Q.M. Khaliq, A fractional-order compartmental model for the spread of the COVID-19 pandemic, Commun. Nonlinear Sci. Numer. Simul. 98 (2021) 105764.
[27] P. Van den Driessche, J. Watmough, Reproduction numbers and sub-threshold endemic equilibria for compartmental models of disease transmission, Math. Biosci. 180 (1–2) (2002) 29–48.
[28] Z. Yaagoub, K. Allali, Fractional HBV infection model with both cell-to-cell and virus-to-cell transmissions and adaptive immunity, Chaos Solitons Fractals 165 (2022) 112855.
[29] J.P.C. dos Santos, E. Monteiro, G.B. Vieira, Global stability of fractional SIR epidemic model, Proc. Ser. Braz. Soc. Comput. Appl. Math. 5 (1) (2017).
[30] Z. Odibat, D. Baleanu, Numerical simulation of initial value problems with generalized Caputo-type fractional derivatives, Appl. Numer. Math. 156 (2020) 94–105.